

**OBSERVATION OF ULF ELECTROMAGNETIC EMISSIONS
BEFORE THE M 7.8 NEW ZEALAND EARTHQUAKE OF NOVEMBER 13, 2016****S.K. Sahoo** ¹✉, **M. Katlamudi** ¹, **G. Udaya Lakshmi**²¹Institute of Seismological Research, Gandhinagar 382009, Gujarat State, India²Osmania University, Hyderabad 500007, Telangana State, India

ABSTRACT. We analyzed the ground geomagnetic data obtained from a 3-component fluxgate magnetometer at the Eyrewell Geomagnetic Observatory (New Zealand) (43.474 °S, 172.393 °E) from October 1 to December 31, 2016. The study aimed to investigate electromagnetic precursors associated with the M 7.8 New Zealand earthquake of November 13, 2016. This earthquake occurred 54 km northeast of Amberley (New Zealand). Its epicenter was located 158 km from the Eyrewell Observatory. We used three methods focused on the polarization ratio, fractal dimension and principal component analysis to identify anomalies in the geomagnetic data. The time series showed an enhanced polarization ratio at two times, October 20 and October 30, 2016, i.e. before the occurrence of the New Zealand earthquake, and a value ~1 or more during these instances. Since the global geomagnetic indices Kp and Dst were normal in these cases, the enhanced polarization ratio may be related to the preparation phase of the New Zealand earthquake. To further classify them, we applied the principal component analysis to the magnetic data on component H. The first three principal components showed more than 90 % of the variance of the original ultra-low frequency (ULF) magnetic field time series. The first principal component was found to be well correlated with the storm index (Dst) recorded during this period. Again, the second principal component was dominated by daily variations, which were the periodic component of the recorded ULF magnetic field. The temporal variation of the third principal component was analyzed to verify a possible correlation between the ULF emissions and the occurrence of the earthquake. The fractal dimension of components D and Z of the magnetic data decreased initially and sharply increased three days before the New Zealand earthquake.

KEYWORDS: ULF; polarization ratio; fractal dimension; earthquakes; Kp; Dst**RESEARCH ARTICLE**

Received: April 26, 2020

Revised: June 8, 2021

Accepted: June 14, 2021

Correspondence: Sushanta Ku Sahoo, sushantageo.sahoo@gmail.com**FOR CITATION:** Sahoo S.K., Katlamudi M., Udaya Lakshmi G., 2021. Observation of ULF electromagnetic emissions before the M 7.8 New Zealand earthquake of November 13, 2016. *Geodynamics & Tectonophysics* 12 (4), 891–901. doi:10.5800/GT-2021-12-4-0561

НАБЛЮДЕНИЕ УЛЬТРАНИЗКОЧАСТОТНЫХ ЭЛЕКТРОМАГНИТНЫХ ИЗЛУЧЕНИЙ ПЕРЕД ЗЕМЛЕТРЯСЕНИЕМ (M=7.8) 13 НОЯБРЯ 2016 Г. В НОВОЙ ЗЕЛАНДИИ

С.К. Саху¹, М. Катламуди¹, Г. Удая Лакшми²

¹ Институт сейсмологических исследований, Гандинагар 382009, штат Гуджарат, Индия

² Османский университет, Хайдарабад 500007, штат Теленгана, Индия

АННОТАЦИЯ. С целью изучения электромагнитных предвестников, связанных с землетрясением 13 ноября 2016 г. в Новой Зеландии, проанализированы наземные геомагнитные данные, полученные с использованием трехкомпонентного магнитометра Геомагнитной обсерватории Эйруэлл (Новая Зеландия) (43.474 ° ю.ш., 172.393 ° в.д.) в период с 1 октября по 31 декабря 2016 г. Землетрясение магнитудой 7.8 балла произошло в 54 км к северо-востоку от г. Эмберли, а его эпицентр находился в 158 км от Геомагнитной обсерватории Эйруэлл. Для выявления аномалий магнитных данных проанализированы коэффициент поляризации, фрактальная размерность и основные компоненты ультранизкочастотного магнитного поля (УНЧ) изучаемого района. По временному ряду коэффициента поляризации установлено, что данный показатель был превышен дважды, а именно 20 и 30 октября 2016 года, т.е. до возникновения землетрясения, и имел значение ~1 и более в этих случаях. Поскольку индексы глобальной геомагнитной активности Кр и Dst были в норме, повышенный коэффициент поляризации мог быть связан с фазой подготовки землетрясения, которое произошло 13 ноября 2016 г. Для дальнейшей классификации проведен анализ основных компонентов магнитного поля. Первые три основных компонента дают более 90 % дисперсии исходного временного ряда магнитного поля УНЧ. Установлено, что первый основной компонент хорошо коррелирует с индексом геомагнитной активности Dst (магнитная буря), зарегистрированным в этот период. При этом во втором главном компоненте преобладали ежедневные колебания, являющиеся периодическим компонентом зарегистрированного магнитного поля УНЧ. Временное изменение третьего основного компонента было проанализировано для проверки возможной корреляции между проявлениями геомагнитных возмущений УНЧ и возникновением землетрясения. Фрактальная размерность D и Z компонентов магнитных данных изначально уменьшилась, но вскоре резко увеличилась. Такие изменения наблюдались за три дня до изучаемого землетрясения.

КЛЮЧЕВЫЕ СЛОВА: УНЧ; коэффициент поляризации; фрактальная размерность; землетрясения; Кр; Dst

1. INTRODUCTION

The proxy related to ultra-low frequency (ULF) magnetic field emissions associated with the earthquakes is becoming more significant among all proxies of earthquake precursors. Many publications have reported a significant increase in ULF emissions before the occurrence of earthquakes [Hayakawa et al., 2007; Hattori, 2004; Rawat, 2014; Chauhan et al., 2012]. Hayakawa et al. [Hayakawa et al., 2007] found the ULF variations related with the tectonic effect during the preparation phase of earthquakes. The ultra-low frequency of <10 Hz was chosen from the wide range of electromagnetic emissions to identify seismic precursors. Although magnetic pulses of various frequencies are generated at an earthquake hypocenter, the ULF signals can propagate a long distance in the lithosphere with small attenuation in comparison to other high frequency signals [Hayakawa et al., 2007]. Akinaga et al. [Akinaga et al., 2001] analyzed the ULF emission data at Luning (epicentral distance 120 km) and found a significant enhancement in the polarization ratio about two months before the M 7.6 Chi-Chi earthquake of September 21, 1999. Many studies have revealed the presence of the electromagnetic (EM) emissions during the earthquake preparation process [Smirnova et al., 2004; Varotsos, 2005; Rawat, 2014; Rawat et al., 2016; Chauhan et al., 2012; Arora et al., 2012; Kumar et al., 2013]. Emerging positive results of studies focused on EM

emission before the earthquakes contribute to searching for a probability of short-term prediction of earthquakes, including forecasting of their locations and time.

The observed Earth's magnetic field is a combination of internal and external sources. The solar wind and the magnetosphere are generally treated as external sources, and the remnant magnetization in the lithosphere/crust is treated as an internal source of the Earth's magnetic field [Mandea, Purucker, 2005]. The ULF waves recorded on the ground carry the characteristics of generation processes and information about the region they have propagated. Abnormal changes in the ULF geomagnetic field associated with seismic activity are due to changes in the magnetic properties of the rock and the electrical conductivity of the crust. Predominantly, in the earthquake precursor studies, the theories of electro-kinetic and piezo-magnetic effects are applied to investigate the origin of the EM field during seismogenic processes. However, no authentic model has been developed yet to explain the seismo-electromagnetic field origin [Pulinets, Boyarchuk, 2004; Yoshida, 2001; Fedorov et al., 2001; Uyeda et al., 2009]. For short-term earthquake prediction studies, two things are most important: (1) Identify the seismo-electromagnetic (SEM) signal from the background EM signals; and (2) Detect the SEM signal position. The presence of a SEM signal can be detected through various analysis protocols such as analysis

of polarization ratio, fractal dimension, principle component analysis, and wavelet. In addition, many scientists are trying to find the source of SEM signals using data from two or more observatories that employ various methods based on phase difference and the polarization ellipse [Schekotov et al., 2008; Dudkin et al., 2010; Hattori, 2004; Hayakawa et al., 2007; Rawat et al., 2016].

The polarization ratio analysis and the fractal dimension analysis were first carried out by Hayakawa et al. [Hayakawa et al., 1996]. He discovered changes in the ULF magnetic field a few days before the earthquake. Many researchers have also indicated that they use the same techniques for identification of the earthquake precursory signals [Gotoh et al., 2004; Smirnova et al., 2004; Varotsos, 2005; Arora et al., 2012; Rawat, 2014]. Before the occurrence of earthquakes, anomalies in magnetic field data were observed by many researchers [Yen et al., 2004; Masci et al., 2009; Chen et al., 2010; Takla et al., 2013]. Moreover, Li et al. [Li et al., 2011] observed abnormality in the 3rd principal component of H-Comp of the magnetic field 40 days before occurrence of the M_s 6.1 Panzihua earthquake (China). Ida Y. and Hayakawa M. [Ida, Hayakawa, 2006] observed anomalous fractal dimensions of the magnetic field 9–14 days before the 1993 Guam earthquake. Rawat et al. [Rawat, 2014] also observed a similar increase in fractal dimensions before local earthquakes in Himalayas (India).

On November 13, 2016, a M 7.8 earthquake occurred at a depth of 15 km in North Canterbury (New Zealand) (42.73 °S, 173.054 °E) (NEIC, USGS). In the present study, we analysed the ground geomagnetic data of a 3-component fluxgate magnetometer (DFM) at Eyrewell (43.474 °S, 172.393 °E) from October 1 to December 31, 2016 to study the electromagnetic precursors associated with this earthquake. We used the polarization ratio, fractal dimension and principal component analysis to identify anomalous magnetic data.

2. TECTONIC SETTING OF THE STUDY AREA

The earthquake occurred in the inter-plate region between the Australian and Pacific plates, that are separated by the Alpine fault. These plates are subjected to oblique convergence at the rates of ~ 36 mm/year and 10 mm/year, respectively [Leitner et al., 2001]. From Jackson Bay to Hope Fault Crossing, the plate boundary is a continent-continent collision zone with the Challenger plateau to the west and the Chatham Rise to the east [Leitner et al., 2001]. The Alpine fault changes in character along the strike zone. From Milford Sound to the Cascade River, it is a steeply dipping strike-slip fault with a very small dip-slip component [Sutherland, Norris, 1995].

The fact behind the frequent occurrence of earthquakes along the northern part with smaller single-event slip compared to the southern part can be related to the Marlborough Fault system or the thermally weakened central section of the Alpine fault, which could make a barrier to southward propagating earthquakes [Leitner et al., 2001].

3. DATA AND METHODOLOGY

In order to study earthquake precursors before the New Zealand earthquake, we analysed the data of a digital fluxgate magnetometer (DFM) installed at the Eyrewell Magnetic Observatory (New Zealand) (43.40 °S, 172.40 °E). The locations of the New Zealand earthquake epicenter and the Observatory are shown in Fig. 1. This station is maintained by the Institute of Geological and Nuclear Sciences and is part of the Intermagnet Network, that promotes high standards of magnetic observatory practice and provides the magnetic data for research purposes (www.intermagnet.org). The magnetic field varies due to the contribution of three different sources, namely the terrestrial-solar activity, the man-made noise and the electromagnetic emissions of the lithosphere through induced microcracks, earthquakes, volcanism etc. It is therefore quite difficult to distinguish

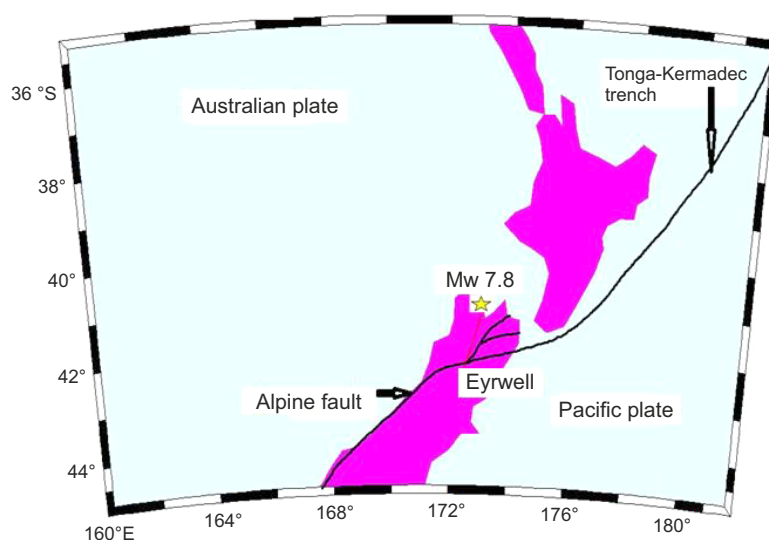


Fig. 1. Location of the epicenter of New Zealand earthquake and the Magnetic Observatory.

Рис. 1. Расположение эпицентра землетрясения 13 ноября 2016 г. ($M=7.8$) и местоположение магнитной обсерватории Эйруэлл (Новая Зеландия).

a weak electromagnetic signal associated with a seismic event from signals generated by other dominating sources in observations of the magnetic field intensity. To reduce the influence of anthropogenic and cultural disturbances, we selected the magnetic data taken at midnight (23:00–02:00 LT) for analysis. We applied the polarization ratio method introduced by [Hayakawa et al., 2007] to detect the earthquake precursor signals in magnetic data. The polarization ratio is Z/G , where Z and G are the vertical and horizontal components of the geomagnetic field, respectively, and $G^2=H^2+D^2$ (H and D are the horizontal components). Our approach is based upon the concept that the influence of the ionosphere and solar terrestrial effect on the Earth’s magnetic field is considered as a far field effect (where it does not carry any vertical component), and the variation due to the influence of the crustal electromagnetic emissions is taken as a near field effect (where the vertical component plays a critical role). Therefore, calculation of the polarization ratio (Z/G) can indicate the source of the geomagnetic field and, thereby, it can assist the information about the contribution of electromagnetic emissions associated with earthquakes [Hayakawa et al., 2007; Hattori, 2004]. In the principal component analysis (PCA), an orthogonal transformation is used to change the correlated variable into uncorrelated variables called principal components. Each principal component of a time series contains specific information

about the salient feature of the original time series. The PCA steps are as follows:

- Let X be a time series having $X=[X_1, X_2, \dots, X_m]$
- The transpose of X is defined as, $X^T=[X_1, X_2, \dots, X_m]^T$
- The variance matrix can be calculated as, $R=XX^T$, and the eigenvalue decomposition of R is given as $R=V\Delta V^T$, where Δ is the eigenvalue matrix with columns λ_1, λ_2 and λ_3 , and V is the eigenvector matrix with columns v_1, v_2 and v_3 .

The PCA main objective is the eigenvalue decomposition of the covariance matrix of the observed time series.

Apart from the above methods, fractal analysis is also an approach by which the dynamics of the earthquake preparation can be studied through variations of fractal dimension (FD) [Rawat, 2014]. The earthquake preparation process is a dynamic process that develops in stages. According to the concept introduced by Bak et al. [Bak et al., 1987], the dynamics of natural hazard systems is based on Self Organizing Criticality (SOC). Here, the occurrence of earthquake is regarded as the critical stage, and the earthquake preparation is considered as the intermediate stage. In the critical stage, the dynamic process is highly sensitive to any type of external perturbations whose time response exhibits the nature of the flicker noise ($1/f$). Hayakawa et al. [Hayakawa et al., 1999] used this technique for the first time in the analysis of ULF data to identify earthquake precursors. Today, three methods are available for FD calculation:

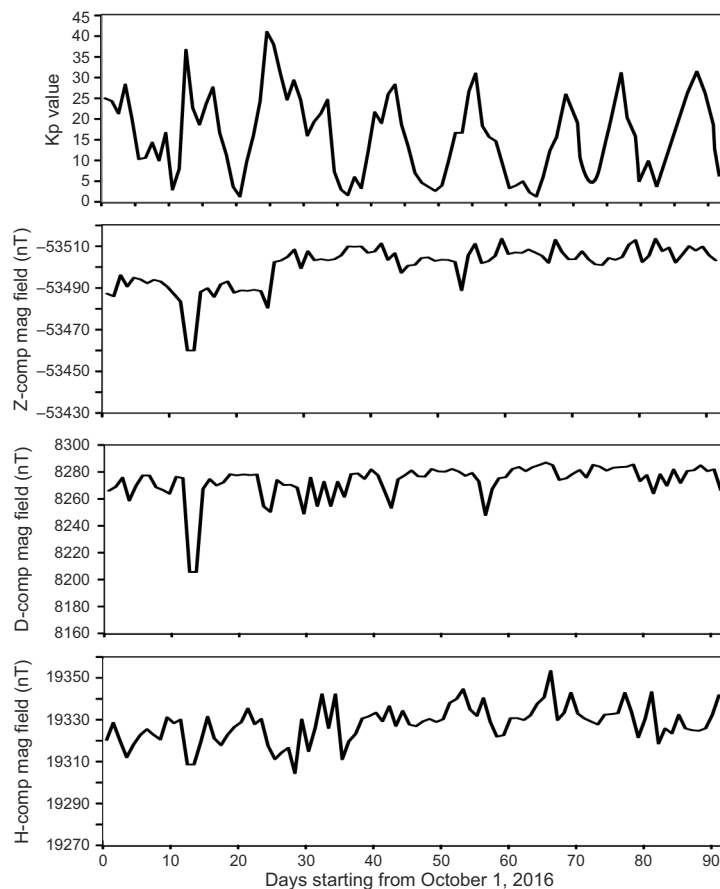


Fig. 2. Kp values and magnetic data of X, Y, Z comp recorded in Eyrewell station.

Рис. 2. Значения индекса геомагнитной активности Kp и магнитных компонентов X, Y, Z по данным обсерватории Эйруэлл.

power spectral density (PSD) method [Berry, 1979], Burlaga-Klein method [Burlaga et al., 1986], and Higuchi method [Higuchi, 1988]. In this study, we used the PSD method as follows:

- Slope β of the behavior of power spectrum $s(f) \propto f^{-\beta}$ is obtained from the line best adjusted in the log-log diagram of the selected frequency band in order to study the behavior characteristic $1/f$;
- The time series is divided into segments with 1024 data points, with 50 % overlapping the previous segment;
- Each segment is subjected to a Fast Fourier transformation.
- The performance spectrum of five segments in 3 hours is then averaged to obtain the most consistent and coherent spectral properties.
- Slope β of the average spectrum is then estimated using a linear fit to the spectrum plotted on a logarithmic scale in

the frequency band from 0.03 to 0.1 Hz. This slope can be linked to the fractal dimension using the Berry equation, $D=(5-\beta)/2$.

The global geomagnetic indices Kp and Dst were obtained from the World Data Center in Kyoto, Japan (<http://wdc.kugi.kyoto-u.ac.jp>). The Kp values and the magnetic data (X, Y, Z components) from the Eyrewell station are shown in Fig. 2.

4. RESULTS AND DISCUSSION

4.1. Anomalies in polarization ratios

Polarization ratios for the far field effect are generally lower than those for the near field effect. The Z/G ratio is less than 1 for the far field effect, however, it is almost equal to 1 or more for the near field effect, considering the electromagnetic emissions from the lithosphere due to micro-cracks or to the electro-kinetic effect associated with the

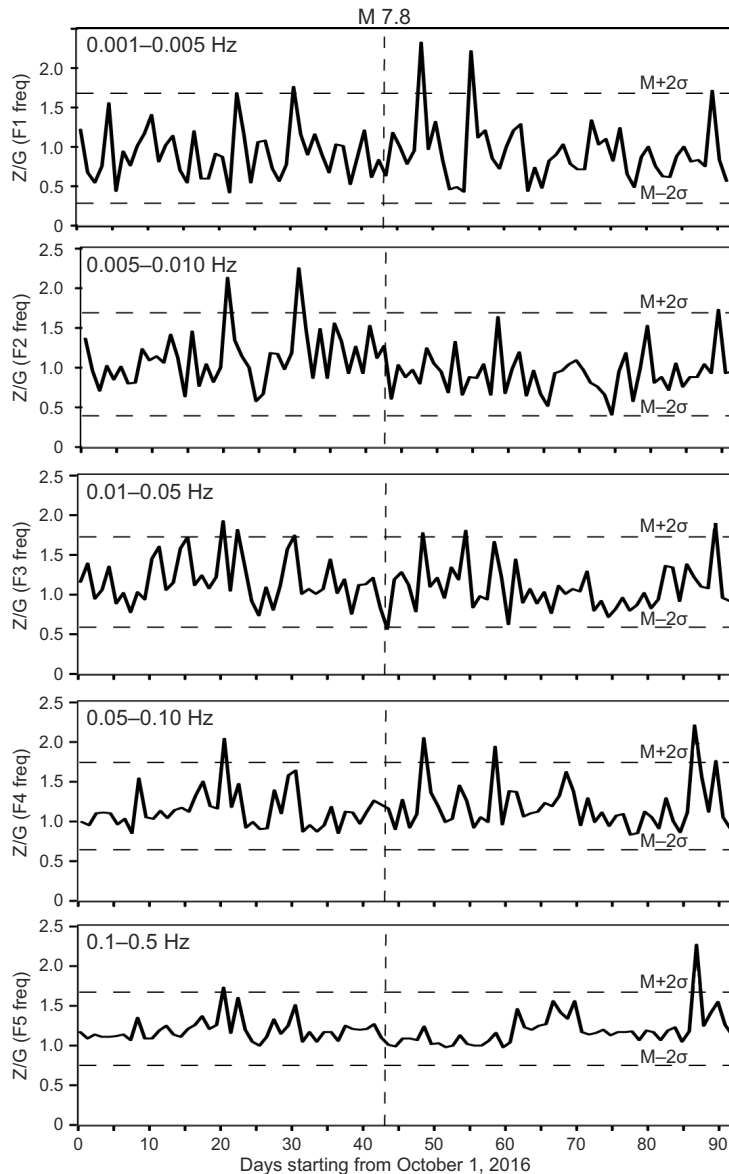


Fig. 3. Plotting of the polarization ratio (Z/G).

Рис. 3. График изменения коэффициента поляризации (Z/G).

occurrence of earthquakes [Hayakawa et al., 2007]. Even though the radio emissions are generated as a pulse in the earthquake hypocenter, higher frequency components cannot propagate over long distances in the lithosphere due to severe attenuation, but ULF waves can propagate up to an observation point near the Earth’s surface with small attenuation. Therefore, an electromagnetic signal in the ULF range was selected for the polarization analysis [Hayakawa et al., 2007]. In our study, the Z/G ratio in the ULF range (0.001–0.5 Hz) was calculated for five frequency bands, i.e. F1 (0.001–0.005 Hz), F2 (0.005–0.01 Hz), F3 (0.01–0.05 Hz), F4 (0.05–0.1 Hz), and F5 (0.1–0.5 Hz), using the data for three months, from October 1 to December 31, 2016 (Fig. 3). The plots showing the temporal evolution of the Z/G ratio for the five frequency bands are based on the records taken at the Eyerell Observatory at midnight (23:00–02:00 LT); the time of the New Zealand earthquake is marked by the dashed line.

Virk et al. [Virk et al., 2001] considered the anomaly in radon time series when the signal exceeded the mean $\pm 2\sigma$. To investigate the abnormal behavior of the polarization ratio, we also applied the mean $\pm 2\sigma$ technique to the polarization ratios of the five frequency bands (shown by dashed lines in Fig. 3). In the first frequency band (F1), peaks appear on October 20, October 30, November 20, November 28,

and December 20, 2016. Frequency band (F2) shows only two large peaks on October 20 and October 30, 2016. Frequency bands (F3) and (F4) show peaks similar to those at (F1), but with lower amplitudes. Frequency band (F5) shows only two peaks, on October 20 and December 20, 2016.

Fig. 4 illustrates the Disturbance Storm Index (Dst) obtained from the World Data Center, Kyoto, Japan (<http://wdc.kugi.kyoto-u.ac.jp>). During the study period, the Dst value varied between -20 and -60, which shows a quiet condition in the ionosphere and no signs of any major magnetic storm.

Most of the peaks occur on the dates preceding and following the date of New Zealand earthquake, i.e. before or after November 13, 2016. The first two peaks – 13 days and 23 days before the New Zealand earthquake – can be considered as the precursors of this earthquake. It is noteworthy that the peaks on October 20 and 30, 2016 are easily detected in all the five frequency bands. Furthermore, there is a remarkable change (>1) in the polarization ratio Z/G from frequency band (F1) to band (F4). In our study, the most characteristic frequency of the seismic ULF emissions vary in the range from 0.005 to 0.1 Hz, which is similar to the results obtained by other researches in their studies of earthquakes in Spitak (Armenia) [Kopytenko et al., 1990], Loma Prieta (California, USA) [Fraser-Smith et al., 1990], Guam

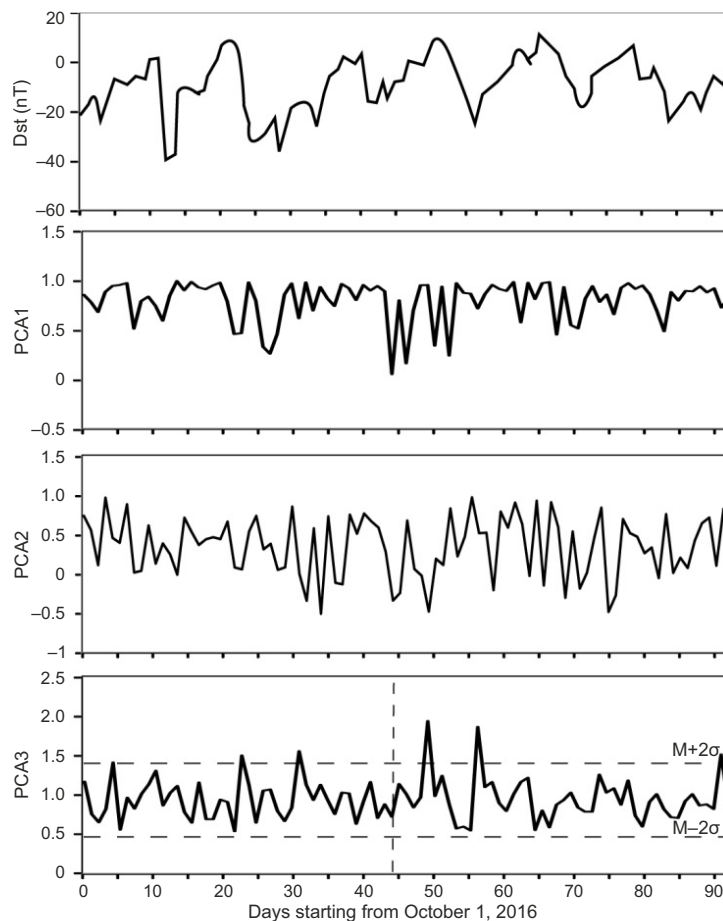


Fig. 4. Principal components of H-component of magnetic field with the Dst.

Рис. 4. Основные компоненты Н магнитного поля с индексом геомагнитной активности Dst.

[Hayakawa et al., 1996], and Biak (Indonesia) [Hayakawa et al., 2000]. In our analysis, the polarization ratio increased significantly at this characteristic frequency from 13 to 23 days before the New Zealand earthquake. Such an increase in the ULF emission is consistent with the value in [Hattori, 2004]. Hayakawa et al. [Hayakawa et al., 2007] assumed that the pre-seismic ULF emissions satisfy the empirical relationship of $0.025R < (M - 4.5)$, where R is epicentral distance and M is magnitude. A relationship with the parameters of the New Zealand earthquake fulfills this empirical relationship, so we can expect a ULF anomaly for this event. The upward trend in the polarization rate continued even after the New Zealand earthquake had occurred, which suggests post-seismic adjustments.

Our observations of the polarization rates are similar to those described in publications on earthquakes in Guam [Hayakawa et al., 1996], Biak (Indonesia) [Hayakawa et al., 2000], northwestern Himalayas (India) [Rawat, 2014], and Chi-Chi (Taiwan) [Hayakawa, 2001]. Various explanations have been proposed for high polarization rates, e.g. (i) an increase in the vertical magnetic field, which can be associated with direct mechanisms acting in the crust, such as micro-fracture electrification [Molchanov, Hayakawa, 1998]; (ii) reduction of the horizontal magnetic field, which can be linked to indirect mechanisms, such as the effects of lithosphere-atmosphere-ionosphere coupling [Gokhberg et al., 1995; Molchanov et al., 2004]; and (iii) inductive seismic-electromagnetic effect [Molchanov et al., 2001]. We cannot exactly relate any one of these mechanisms in the case of the New Zealand earthquake. Nonetheless, the propagation of EM emissions generated by one of these mechanisms is easily detectable in this case because the observation station is located so close to the epicenter of the New Zealand earthquake.

4.2. Anomalies in principal components

Various authors have successfully used the principal component analysis (PCA) in various fields, e.g. [Labib, Vemuri, 2004] – computer networks to facilitate traffic analysis and visualization; [Quershi et al., 2017] – medical data to study heart disease risks; [Alken et al., 2017] – ionosphere data to characterize the equatorial and Sq electrojet power systems; and [Hayakawa et al., 2007] – investigations of ULF variations related to earthquakes.

As mentioned above, variations in the geomagnetic field can be due to the contributions of the three sources, namely the terrestrial-solar activity, the man-made noise, and the electromagnetic emissions of the Earth. In the context of earthquakes, volcanism, etc., the PCA analysis plays a crucial role in determining the real source of the magnetic field. Since the source of the terrestrial-solar component does not have the vertical component, the PCA analysis of the horizontal components can determine the real source of variations in the magnetic field. In this study, we used the H component for the PCA analysis. Fig. 5 illustrates the three principal components with Dst values in the period from October 1 to December 31, 2016. The variation of the eigenvalue of the first principal component is strongly correlated with the Dst value compared to the two other components. We may assume that the first principal component of the observed signal is due to the contribution of the global magnetic signal resulting from the terrestrial-solar activity. The eigenvalue of the second main component shows a daily variation (24 hours) during the study period with maximum and minimum values of day and night, respectively (Fig. 5). Therefore, it is also considered to be an influence of periodic components. Fig. 5 shows the temporal evolution of the eigenvalue of the third principal component during the study period. This value is increased on October 20,

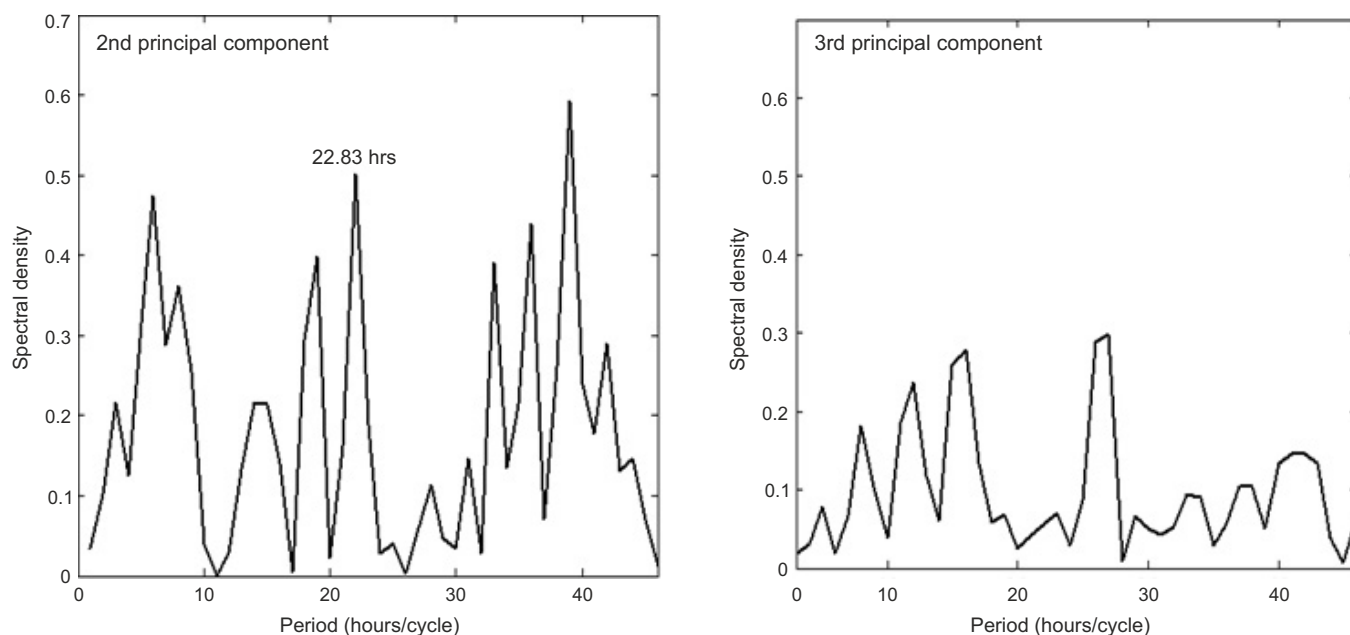


Fig. 5. FFT periodograms of the 2nd and 3rd principal components.

Рис. 5. Периодограммы 2-го и 3-го основных компонентов, полученные с применением быстрого преобразования Фурье (FFT).

October 30, November 20, November 28 and December 20, 2016. These increases correlate with the enhancements of polarization ratios described above. The enhancements on October 20 and October 30, 2016 can be related to the electromagnetic emissions due to microfracturing during the preparation phase of the New Zealand earthquake. An increase in the third principal component several days before other earthquakes is reported in the following publications: [Hattori, 2004] – the Izu earthquake; [Serita et al., 2005] – earthquakes in Japan; [Hayakawa et al., 2007] – earthquakes on the Izu and Boso peninsulas; and [Li et al., 2011] – earthquakes in the Pranzhuhua region of China.

4.3. Anomalies in fractal dimensions

We calculated fractal dimensions (FD) by applying the Berry method to components H, D and Z of the magnetic field from October 1 to December 31, 2016 to search for anomalies before the New Zealand earthquake. Fig. 6 shows

FD calculation for a single day; (a) the time series of magnetic data for 18–21 hours at a one-second sampling interval; (b) an amplitude spectrum (we applied the FFT to this time series); and (c) a robust least squares adjustment of the straight line, which is applied to the log-log scale. The slope β of the average spectrum is estimated in the frequency band of 0.03–0.1 Hz. A corresponding FD value (D) is obtained from the Berry equation using the slope β for the three components every day. In this way, we calculate FD of three orthogonal components of the variations of the geomagnetic field, which makes it possible to obtain three sequences of the FD temporal variations corresponding to components X (NS), Y (EW), and Z (vertical).

Fig. 7 shows the FD time evolution of the geomagnetic components (H, D, and Z) and the Dst value. The three components differ in the FD variability, that is higher for components Y and Z and comparatively lower for component X. We observe that the FD of component H fluctuates widely,

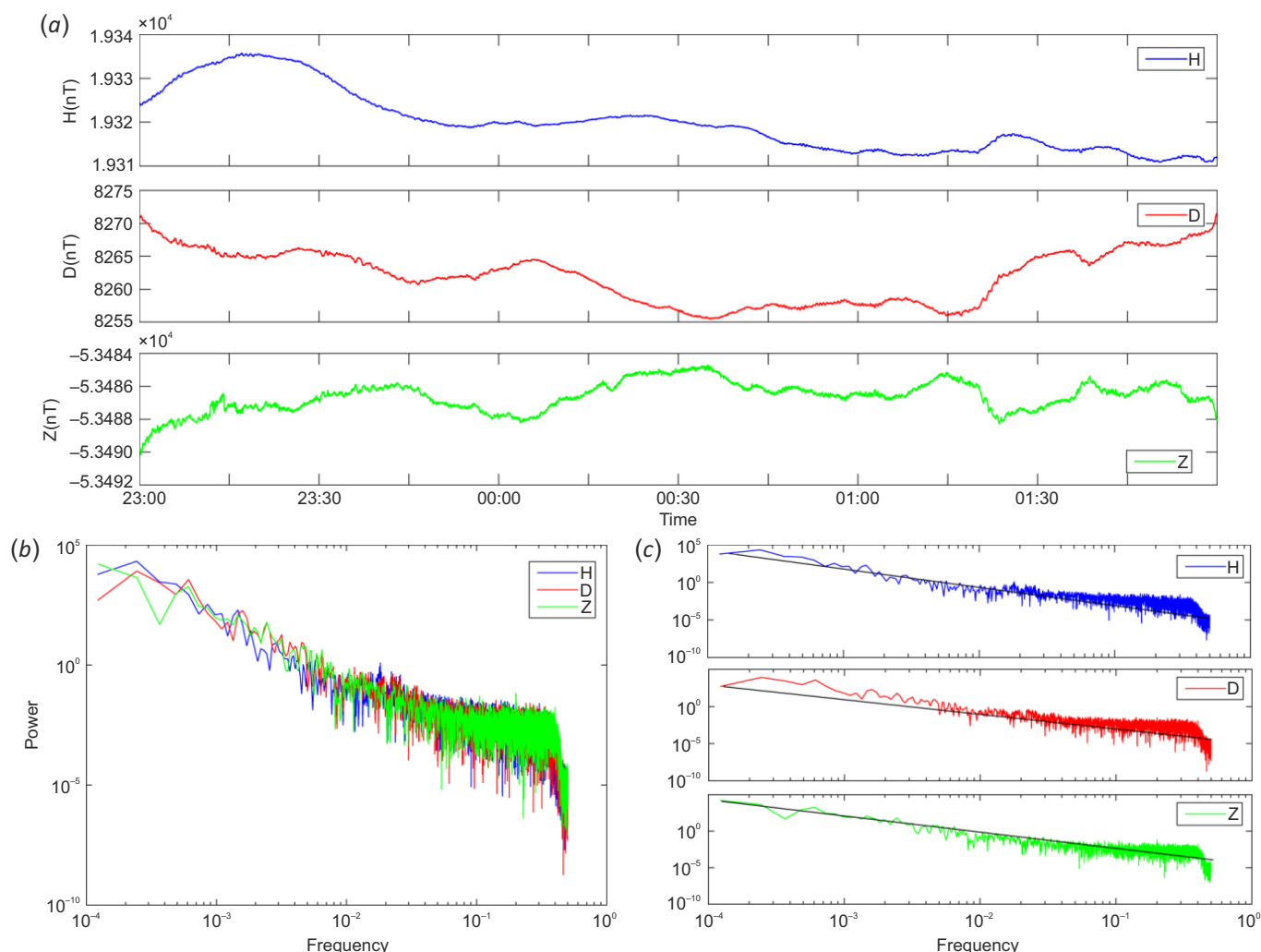


Fig. 6. Estimation of the slope of the power spectra.

(a) – the time series of the geomagnetic field during night-time; (b) – the power spectra of all the three components (H, D and Z); (c) – log-log fitting of the straight line.

Рис. 6. Расчет наклона спектров мощности.

(a) – временной ряд геомагнитного поля в ночное время; (b) – спектры мощности всех трех компонентов (H, D и Z); (c) – логарифмическая кривая, соответствующая прямой линии.

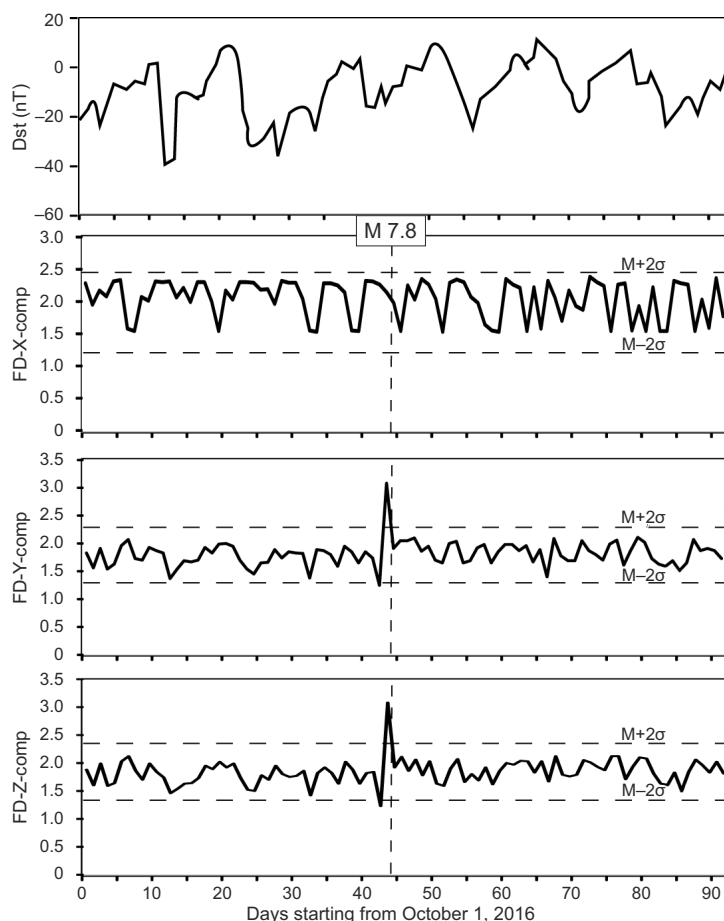


Fig. 7. Fractal dimension variability determined by Berry's method during October 1 to December 31, 2016.

Рис. 7. Изменчивость фрактальной размерности, определенная методом Берри в период с 1 октября по 31 декабря 2016 г.

and it is therefore too difficult to obtain a temporal evolution of this component. For components D and Z, however, the FD variation follows a certain trend. During the study period, an average FD value of components D and Z is 1.8. The FD value of components D and Z decreases below the average on November 10, 2016, but is restored and immediately increased on the same day, November 10, 2016, i.e. three days before the New Zealand earthquake. This increase in the fractal dimension can therefore be linked to the seismic preparation processes of the New Zealand earthquake of November 13, 2016. An increase in the fractal dimension before other earthquakes is reported in the following publications: [Gotoh et al., 2003] – the August 8, 1993 earthquake on the island of Guam; [Ida et al., 2012] – earthquakes in China; [Rawat, 2014] – the Himalayan earthquake; [Han et al., 2015] – the 2009 LAquila earthquake in Italy; [Rawat et al., 2016] – local earthquakes in the Ghuttu region of India. Considering the increase in the fractal dimension before the New Zealand earthquake, as established in our study, we confirm the effect of a decrease in the ULF emission spectrum slope before the earthquake.

5. CONCLUSION

Based on the above data, we identified anomalies in the magnetic data from the Eyrewell Observatory before the

occurrence of the M 7.8 New Zealand earthquake of November 13, 2016. Since this earthquake occurred at a distance of 158 km from the Eyrewell Observatory, we were able to clearly detect the precursory signals in the three-components magnetic data. To identify the anomalies, we used three methods focused on the polarization ratio, fractal dimension and principal component analysis. All the five frequency bands of the polarization ratio showed anomalies on October 20 and October 30, 2016. Similarly, we also observed the anomalies on October 20 and October 30, 2016 in the third principal component (H) of the magnetic data. The fractal dimension of components D and Z of the magnetic data initially decreased and sharply increased three days before the New Zealand earthquake. By systematically analyzing 3-component magnetic data using the polarization ratio, the principal component and the fractal dimension, we can confidently conclude that electromagnetic precursors of earthquakes can contribute to deciphering the code of the various Earth signals before the earthquakes.

6. ACKNOWLEDGEMENT

The results presented in this article are based on the magnetic data of the Eyrewell Geomagnetic Observation (New Zealand). We thank the Institute of Geology and Nuclear Sciences for the operation of this station and the availability

of magnetic data. Our special thanks go to INTERMAGNET for promoting high standards in the practice of magnetic observatories (www.intermagnet.org). The authors thank the Director General of the Institute of Seismological Research, Department of Science and Technology, Government of Gujarat, for his encouragement to carry out the work. The authors would like to thank Marina Pochekunina, Managing Editor of Geodynamics & Tectonophysics Journal and two anonymous reviewers for constructive suggestions which markedly improved the paper.

7. REFERENCES

- Akinaga Y., Hayakawa M., Liu J.Y., Yumoto K., Hattori K., 2001. A Precursory ULF Signature for the Chi-Chi Earthquake in Taiwan. *Natural Hazards and Earth System Sciences* 1 (1/2), 33–36. <https://doi.org/10.5194/nhess-1-33-2001>.
- Alken P., Maute A., Richmond A.D., Vanhamäki H., Egbert G.D., 2017. An Application of Principal Component Analysis to the Interpretation of Ionospheric Current Systems. *Journal of Geophysical Research: Space Physics* 122 (5), 5687–5708. <https://doi.org/10.1002/2017JA024051>.
- Arora B.R., Rawat G., Kumar N., Choubey V.M., 2012. Multi-Parameter Geophysical Observatory: Gateway to Integrated Earthquake Precursory Research. *Current Science* 103 (11), 1286–1299.
- Bak P., Tang C., Wiesenfeld K., 1987. Self-Organized Criticality: An Explanation of $1/f$ Noise. *Physical Review Letters* 59 (4), 381–384. <https://doi.org/10.1103/PhysRevLett.59.381>.
- Berry M.V., 1979. Diffractals. *Journal of Physics A: Mathematical and General* 12 (6), 207–220.
- Burlaga L.F., Klein L.W., 1986. Fractal Structure of the Interplanetary Magnetic Field. *Journal of Geophysical Research: Space Physics* 91 (A1), 347–350. <https://doi.org/10.1029/JA091iA01p00347>.
- Chauhan V., Pandey U., Singh B., Arora B.R., Rawat G., Pathan B.M., Sinha A.K., Sharma A.K., Patil A.V., 2012. A Search for Precursors of Earthquakes from Multi-Station ULF Observations and TEC Measurements in India. *Indian Journal of Radio and Space Physics* 41, 543–556.
- Chen C.-H., Liu J.-Y., Lin P.-Y., Yen H.-Y., Hattori K., Liang W.-T., Zeng X., 2010. Pre-Seismic Geomagnetic Anomaly and Earthquake Location. *Tectonophysics* 489 (1–4), 240–247. <https://doi.org/10.1016/j.tecto.2010.04.018>.
- Dudkin F., Rawat G., Arora B.R., Korepanov V., Leontyeva O., Sharma A.K., 2010. Application of Polarization Ellipse Technique for Analysis of ULF Magnetic Fields from Two Distant Stations in Koyna-Warna Seismoactive Region, West India. *Natural Hazards and Earth System Sciences* 10 (7), 1513–1522. <https://doi.org/10.5194/nhess-10-1513-2010>.
- Fedorov E., Pilipenko V., Uyeda S., 2001. Electric and Magnetic Fields Generated by Electrokinetic Processes in a Conductive Crust. *Physics and Chemistry of the Earth, Part C: Solar, Terrestrial & Planetary Science* 26 (10–12), 793–799. [https://doi.org/10.1016/S1464-1917\(01\)95027-5](https://doi.org/10.1016/S1464-1917(01)95027-5).
- Fraser-Smith A.C., Bernardi A., McGill P.R., Ladd M.E., Helliwell R.A., Villard Jr.A.D., 1990. Low-Frequency Magnetic Field Measurements near the Epicenter of the M_s 7.1 Loma-Prieta Earthquake. *Geophysical Research Letters* 17 (9), 1465–1468. <https://doi.org/10.1029/GL017i009p01465>.
- Gokhberg M.B., Morgounov V.A., Pokhotelov O.A., 1995. *Earthquake Prediction: Seismo-Electromagnetic Phenomena*. Gordon & Breach, Australia, USA, 193 p.
- Gotoh K., Hayakawa M., Smirnova N., 2003. Fractal Analysis of the ULF Geomagnetic Data Obtained at Izu Peninsula, Japan in Relation to the Nearly Earthquake Swarm of June–August 2000. *Natural Hazards and Earth System Sciences* 3 (3/4), 229–236. <https://doi.org/10.5194/nhess-3-229-2003>.
- Gotoh K., Hayakawa M., Smirnova N., Hattori K., 2004. Fractal Analysis of Seismogenic ULF Emissions. *Physics and Chemistry of the Earth, Parts A/B/C* 29 (4–9), 419–424. <https://doi.org/10.1016/j.pce.2003.11.013>.
- Han Q., Carpinteri A., Lacidogna G., Xu J., 2015. Fractal Analysis and Yule Statistics for Seismic Prediction Based on 2009 L'Aquila Earthquake in Italy. *Arabian Journal of Geosciences* 8, 2457–2465. <https://doi.org/10.1007/s12517-014-1386-y>.
- Hattori K., 2004. ULF Geomagnetic Changes Associated with Large Earthquakes. *Terrestrial, Atmospheric and Oceanic Sciences* 15 (3), 329–360. [https://doi.org/10.3319/TAO.2004.15.3.329\(EP\)](https://doi.org/10.3319/TAO.2004.15.3.329(EP)).
- Hayakawa M., 2001. *NASDA's Earthquake Remote Sensing Frontier Research. Seismo-Electromagnetic Phenomena in the Lithosphere, Atmosphere and Ionosphere*. Final Report. University of Electro-Communications, Tokyo, 228 p.
- Hayakawa M., Hattori K., Ohta K., 2007. Monitoring of ULF (Ultra-Low-Frequency) Geomagnetic Variation Associated with Earthquakes. *Sensors* 7 (7), 1108–1122. <https://doi.org/10.3390/s7071108>.
- Hayakawa M., Ito T., Hattori K., Yumoto K., 2000. ULF Electromagnetic Precursors for an Earthquake at Biak, Indonesia on 17 February, 1996. *Geophysical Research Letters* 27 (10), 1531–1534. <https://doi.org/10.1029/1999GL005432>.
- Hayakawa M., Kawate R., Molchanov O.A., Yumoto K., 1996. Results of Ultra-Low-Frequency Magnetic Field Measurements during the Guam Earthquake of 8 August, 1993. *Geophysical Research Letters* 23 (3), 241–244. <https://doi.org/10.1029/95GL02863>.
- Hayakawa M., Tetsuya I., Smirnova N., 1999. Fractal Analysis of ULF Geomagnetic Data Associated with the Guam Earthquake on August 8, 1993. *Geophysical Research Letters* 26 (18), 2797–2800. <https://doi.org/10.1029/1999GL005367>.
- Higuchi T., 1988. Approach to an Irregular Time Series on the Basis of the Fractal Theory. *Physica D: Nonlinear Phenomena* 31 (2), 277–283. [https://doi.org/10.1016/0167-2789\(88\)90081-4](https://doi.org/10.1016/0167-2789(88)90081-4).
- Ida Y., Hayakawa M., 2006. Fractal Analysis for the ULF Data during the 1993 Guam Earthquake to Study Prefractal Criticality. *Nonlinear Processes in Geophysics* 13 (4), 409–412. <https://doi.org/10.5194/npg-13-409-2006>.
- Ida Y., Yang D., Li Q., Sun H., Hayakawa M., 2012. Fractal Analysis of ULF Electromagnetic Emissions in Possible

Association with Earthquakes in China. *Nonlinear Processes in Geophysics* 19 (5), 577–583. <https://doi.org/10.5194/npg-19-577-2012>.

Kopytenko Yu.A., Matiashvili T.G., Voronov P.M., Kopytenko F.A., Molchanov O.A., 1990. Ultra Low Frequency Emissions Associated with Spitak Earthquake and Following Aftershock Activity using Geomagnetic Pulsation Data at Observatories Dusheti and Vordziya. Preprint of IZMIRAN N3(888).

Kumar N., Rawat G., Choubey V.M., Hazarika D., 2013. Earthquake Precursory Research in Western Himalaya Based on the MPGO Data. *Acta Geophysica* 61, 977–999. <https://doi.org/10.2478/s11600-013-0133-1>.

Labib K., Vemuri V.R., 2004. An Application of Principal Component Analysis to the Detection and Visualization of Computer Network Attacks. *Annales Des Télécommunications* 61, 218–234. <https://doi.org/10.1007/BF03219975>.

Leitner B., Eberhart-Phillips D., Anderson H., Nabelek J.L., 2001. A Focused Look at the Alpine Fault, New Zealand: Seismicity, Focal Mechanisms, and Stress Observations. *Journal of Geophysical Research: Solid Earth* 106 (B2), 2193–2220. <http://doi.org/10.1029/2000JB900303>.

Li J., Li Q., Yang D., Wang X., Hong D., He K., 2011. Principal Component Analysis of Geomagnetic Data for the Panzihua Earthquake (Ms 6.1) in August 2008. *Data Science Journal* 10, IAGA130–IAGA138. <http://doi.org/10.2481/dsj.IAGA-20>.

Mandea M., Purucker M., 2005. Observing: Modeling, and Interpreting Magnetic Fields of the Solid Earth. *Surveys in Geophysics* 26, 415–459. <https://doi.org/10.1007/s10712-005-3857-x>.

Masci F., Palangio P., Di Persio M., 2009. Magnetic Anomalies Possibly Linked to Local Low Seismicity. *Natural Hazards and Earth System Sciences* 9 (5), 1567–1572. <https://doi.org/10.5194/nhess-9-1567-2009>.

Molchanov O., Fedorov E., Schekotov A., Gordeev E., Chebrov V., Surkov V., Rozhnoi A., Andreevsky S. et al., 2004. Lithosphere-Atmosphere-Ionosphere Coupling as Governing Mechanism for Preseismic Short-Term Events in Atmosphere and Ionosphere. *Natural Hazards and Earth System Sciences* 4, 757–767. <https://doi.org/10.5194/nhess-4-757-2004>.

Molchanov O.A., Hayakawa M., 1998. On the Generation Mechanism of ULF Seismogenic Electromagnetic Emissions. *Physics of the Earth and Planetary Interiors* 105 (3–4), 201–210. [https://doi.org/10.1016/S0031-9201\(97\)0091-5](https://doi.org/10.1016/S0031-9201(97)0091-5).

Molchanov O., Kulchisky A., Hayakawa M., 2001. Inductive Seismo-Electromagnetic Effect in Relation to Seismogenic ULF Emission. *Natural Hazards and Earth System Sciences* 1 (1/2), 61–67. <https://doi.org/10.5194/nhess-1-61-2001>.

Pulinets S.A., Boyarchuk K.A., 2004. *Ionospheric Precursors of Earthquakes*. Springer, Berlin, 315 p. <https://doi.org/10.1007/b137616>.

Quereshi N.A., Suthar V., Magsi H., Sheikh M.J., Pathan M., Qureshi B., 2017. Application of Principal Component Analysis

to Medical Data. *Indian Journal of Science and Technology* 10 (20), 1–9. <https://doi.org/10.17485/ijst/2017/v10i20/91294>.

Rawat G., 2014. Characteristics ULF Band Magnetic Variations at MPGO, GHUTTU for the 20 June, 2011 Earthquake in Garhwal Himalaya. *Current Science* 106 (1), 88–93.

Rawat G., Chauhan V., Damodharan S., 2016. Fractal Dimension Variability in ULF Magnetic Field with Reference to Local Earthquakes at MPGO, Ghuttu. *Geomatics, Natural Hazards and Risk* 7 (6), 1937–1947. <https://doi.org/10.1080/19475705.2015.1137242>.

Schekotov A.Y., Molchanov O.A., Hayakawa M., Fedorov E.N., Chebrov V.N., Sinititsin V.I., Gordeev E.E., Andreevsky S.E. et al., 2008. About Possibility to Locate an EQ Epicenter Using Parameters of ELF/ULF Preseismic Emission. *Natural Hazards and Earth System Sciences* 8 (6), 1237–1242. <https://doi.org/10.5194/nhess-8-1237-2008>.

Serita A., Hattori K., Yoshino C., Hayakawa M., Isezaki N., 2005. Principal Component Analysis and Singular Spectrum Analysis of ULF Geomagnetic Data Associated with Earthquakes. *Natural Hazards and Earth System Sciences* 5 (5), 685–689. <https://doi.org/10.5194/nhess-5-685-2005>.

Smirnova N., Hayakawa M., Gotoh K., 2004. Precursory Behavior of Fractal Characteristics of the ULF Electromagnetic Fields in Seismic Active Zones before Strong Earthquakes. *Physics and Chemistry of the Earth* 29 (4–9), 445–451. <https://doi.org/10.1016/j.pce.2003.11.016>.

Sutherland R., Norris R.J., 1995. Late Quaternary Displacement Rate, Paleoseismicity, and Geomorphic Evolution of the Alpine Fault: Evidence from Hokuri Creek, South Westland, New Zealand. *New Zealand Journal of Geology and Geophysics* 38 (4), 419–430. <https://doi.org/10.1080/00288306.1995.9514669>.

Takla E.M., Yumoto K., Okano S., Uozumi T., Abe S., 2013. The Signature of the 2011 Tohoku Mega Earthquake on the Geomagnetic Field Measurements in Japan. *NRIAG Journal of Astronomy and Geophysics* 2 (2), 185–195. <https://doi.org/10.1016/j.nrjag.2013.08.001>.

Uyeda S., Kamogawa M., Nagao T., 2009. Short-Term Earthquake Prediction: Current Status of Seismo-Electromagnetics. *Tectonophysics* 470 (3–4), 205–213. <http://dx.doi.org/10.1016/j.tecto.2008.07.019>.

Varotsos P.A., 2005. *The Physics of Seismic Electric Signals*. TERRAPUB, Tokyo, 338 p.

Virk H.S., Walia V., Kumar N., 2001. Helium/Radon Precursory Anomalies of Chamoli Earthquake, Garhwal Himalaya, India. *Journal of Geodynamics* 31 (2), 201–210. [https://doi.org/10.1016/S0264-3707\(00\)00022-3](https://doi.org/10.1016/S0264-3707(00)00022-3).

Yen H.-Y., Chen C.-H., Yeh Y.-H., Liu J.-Y., Lin C.-R., Tasi Y.-B., 2004. Geomagnetic Fluctuations during the 1999 Chi-Chi Earthquake in Taiwan. *Earth Planets Space* 56, 39–45. <https://doi.org/10.1186/BF03352489>.

Yoshida S., 2001. Convection Current Generated Prior to Rupture in Saturated Rocks. *Journal of Geophysical Research: Solid Earth* 106 (B2), 2103–2120. <https://doi.org/10.1029/2000JB900346>.